Research

Article submitted to journal

Subject Areas:
systems biology, microbiology, physiology

Keywords:
Cellular heterogeneity, *Aspergillus niger*, enzymatic degradation, specialisation and optimisation, multi-step processes, compartmentalisation

Author for correspondence:
Eric Siero
e-mail: eric.siero@wur.nl

Employment of self-organisation to achieve economy of scale in biology

Eric Siero[1,2], Eva Slegers[3], Koen Herman[3] and Robert-Jan Bleichrodt[3]

[1]Department of Plant Sciences, Biometris, Wageningen University and Research, Wageningen, The Netherlands.
[2]Department of Earth Sciences, Geosciences, Utrecht University, Utrecht, The Netherlands.
[3]Microbiology, Department of Biology, Utrecht University, Utrecht, The Netherlands.

Self-organisation is a striking phenomenon that fascinates many. Especially in homogeneous environments, the question why - and how - heterogeneous structure emerges is intriguing. We find a novel function of self-organisation in biology at the colony margin of the fungus *Aspergillus niger*. Here, the collection of interconnected hyphae splits into two sub-populations with differential expression of amylolytic enzymes. These enzymes are secreted and together break down starch in a multi-step process.

We show with a mathematical model that concentrating production and secretion of all enzymes by part of the hyphae results in more efficient substrate degradation, as compared to equal distribution over all hyphae. This model result is corroborated by experimental observations of increased metabolic activity of the wild type that displays hyphal heterogeneity as compared to a mutant that lost this heterogeneity.

The intermediate product (iso)maltose is known to induce upregulation of amylolytic enzymes. Incorporating this in the model enables the formation of hyphal heterogeneity through self-organisation. We generalize our results to a large class of multi-step processes and demonstrate wide applicability. Importantly, this shows that self-organisation may not be incidental, but favorable and thus selectable since it enhances efficiency. Due to its impact on system functioning, its study is not only of academic interest but also of practical value.

1. Introduction

The mycelium of filamentous fungi consists of an interconnected network of hyphae. Individual hyphae extend at their apices by polarized growth and branch subapically [1,2]. Filamentous growth allows fungi to rapidly explore and colonize various organic substrates, such as lignocellulose and starch [3]. This makes fungi key players in global nutrient recycling as well as notorious food spoilage agents. Moreover, they are utilized as cell factories for the production of enzymes and organic acids.

Starch is the most abundant plant storage carbohydrate. For instance, many crops produce starch storing organs, such as cereals, tubers, roots, and beans [4]. Starch granules consist of amylose, a linear glucan polymer, and amylopectin, which is a highly branched glucan polymer. Fungi secrete a variety of starch degrading enzymes divided over three functional groups of the Glycoside Hydrolase (GH) families [5]. These enzymes hydrolyze starch synergistically to ultimately produce glucose. α-amylases GH13 (EC 3.2.1.1) endolytically hydrolyze α-1,4 linkages in amylose (α-1,4-glucan) chains, breaking up amylose into smaller glucose polymers and maltooligosaccharides. Glucoamylases GH15 (EC 3.2.1.3) and α-glucosidases GH31 (EC 3.2.1.20) exolytically hydrolyze α-1,4 linkages from non-reducing ends, releasing glucose of β-anomeric and α-anomeric forms, respectively. Glucoamylases also hydrolyze α-1,6 linkages at the branch connections in amylopectin [6]. Since we focus this paper on amylose degradation as example, degradation of amylopectin is not further described here.

In *Aspergillus*, expression of the amylolytic genes is tightly regulated. The production of amylolytic enzymes is induced by (iso)maltose through activation of the transcriptional regulator AmyR which then transits to the nucleus [7] and binds to the promotors of amylolytic genes which activate transcription [8]. Thus, three enzyme families work in concert to break down amylose polymers to its constituent glucose monomers. Subsequently, these monomeres pass through sugar transporter transmembrane proteins [9] and are further catabolized. We refer to both the enzymes and the transporters as catalysts.

Previously, the mycelium was regarded as homogeneous, but over the past decades heterogeneity has been established at multiple levels [10–13]. Hyphae of filamentous fungi are compartmentalized by cross walls. These septa have a central pore that can be plugged by Woronin bodies [14,15]. Septal plugging allows fungi to develop hyphal heterogeneity, by containing local gene expression, while still providing control over selective transport between compartments [16,17].

This was first observed for heterogeneous expression of *glaA* (glucoamylase) in leading hyphae of *A. niger* [11], where environmental conditions are arguably identical [11,13,18]. Two subpopulations of hyphae, either highly or lowly expressing GFP under control of the *glaA* promoter, were identified based on fluorescence intensity. This was substantiated by the observation that additional regulatory and amylolytic enzyme encoding genes follow the same expression pattern as *glaA*, i.e. *amyR* and *aamA* (α-amylase), respectively [13]. Moreover, hyphae highly expressing *glaA* also contain a higher abundance of 18S rRNA, indicating a higher translational activity. Taken together, this indicates that at least two subpopulations of hyphae exist in the colony margin, having either high- or low transcriptional and translational activity. Notably, despite the different behavior, both subpopulations display similar growth rates during normal conditions [13].

It is currently not fully clear how and why filamentous fungi develop hyphal heterogeneity [19]. Previously, this phenomenon has been attributed to stochastic processes that introduce diversity within the hyphal population [11], serving as a bet-hedging strategy to enhance survival under adverse conditions [20]. Through mathematical modeling, we demonstrate that hyphal heterogeneity significantly enhances the efficiency of enzymatic starch degradation. This model prediction is corroborated by metabolic measurements comparing wild type (heterogeneous hyphae) and mutant (homogeneous hyphae) strains: heterogeneous hyphae exhibit higher metabolic activity. Extension of our model with upregulation of amylolytic

enzyme concentrations via *amyR*, induced by (iso)maltose, facilitates self-organisation of hyphal heterogeneity. This finding indicates that only minimal regulatory parameters are required to improve the efficiency of the multi-step enzymatic process.

2. Methods

(a) Mathematical model

Degradation of amylose by the fungus *Aspergillus niger* can be viewed as a chain of catalysed reactions. We built a concise model in which amylose, oligosaccharides, external and internal glucose are represented by P_1, P_2, P_3 and P_4 respectively - thus avoiding having to keep track of all polysaccharide concentrations separately. The actors A_i that catalyse the conversion from P_i to P_{i+1} are α-amylase (A_1), glucoamylase combined with α-glucosidase (A_2) and glucose transporter (A_3). The concentrations of the products P_i and catalysts A_i are denoted by p_i and α_i, respectively. The amylolytic process and mathematical model are depicted in Fig. 1. Our qualitative results do not depend on the choice of model parameters unless stated otherwise. For simplicity, we set all parameters equal to 1 (our qualitative results will not depend on their values), except for the catalyst concentrations α_i which are allowed to vary between 0 and 2. Model equations and sensitivity analysis can be found in the electronic supplementary material, with in Fig. 5A a more extensive model including the regulatory network.

(b) Strains and culture conditions

Aspergillus niger N402 was used as a control strain, exhibiting heterogeneous gene expression. The strain N402*ΔhexA* with an inactivation of *hexA*, resulting in the elimination of Woronin bodies, was used as a strain exhibiting no heterogeneous gene expression [20].

To obtain spores, both strains were grown for 7 days on complete medium (minimal medium (MM) [24] with 0.2% tryptone, 0.1% casamino acids, 0.1% yeast extract, 0.05% yeast ribonucleic acids) supplemented with 1% glucose. Spores were harvested in saline tween (ST) (0.9% NaCl (w/v), 0.005% Tween-20 (v/v)) and counted with a haemocytometer and further diluted to a concentration of 5×10^5 spores ml^{-1} in ST.

The strains were grown as sandwich colonies [10] to prevent sporulation and to allow transfer to inducing medium. The sandwich colonies were placed on top of MM agar medium supplemented with $200\ \mathrm{mM}$ xylose in a $9\ \mathrm{cm}$ Petri dish, to repress amylolytic gene expression. To this end, one membrane (polycarbonate membrane, diameter $76\ \mathrm{mm}$, pore sixe $0.1\ \mu\mathrm{m}$; Osmonics, GE Water Technologies, Trevose, PA, USA) was placed on the medium. Thereafter, a $20\ \mu\mathrm{l}$ drop of 1.25% agarose was placed on the center of the membrane. After solidification, $2\ \mu\mathrm{l}$ of the spore solution (5×10^5 spores ml^{-1}) was placed on the agarose and allowed to dry and germinate overnight at $30\ ^\circ\mathrm{C}$. Then, the second membrane was placed. Sandwich colonies were incubated at $30\ ^\circ\mathrm{C}$ for an additional 4 days. Subsequently, the sandwich colonies were transferred onto MM agar medium supplemented with 2% starch, to induce amylolytic activity. The colonies were placed back at $30\ ^\circ\mathrm{C}$ for 8 or 24 hours. After the removal of the sandwich colonies, Lugol staining was performed with $10\ \mathrm{ml}$ Lugol solution for 10 min (Iodine/Potassium iodide solution, Fluka) to detect starch. Subsequently, the plates were washed three times with $10\ \mathrm{ml}$ phosphate-buffered saline (PBS) to remove excess staining solution.

(c) CO_2 and biomass measurements

Carbon dioxide production for each colony was measured every 20 seconds during 3 minutes after amylolytic genes had been induced for 8 h on starch. The measurements were carried out in septuplicate. To this end, one culture was placed at a time in a clear airtight box (Modula $2000\ \mathrm{ml}$, Mepal) together with a battery powered bespoke CO_2 data logger inside. The box was closed to allow CO_2 building up. The data logger was produced by connecting a SCD41 CO_2 sensor to

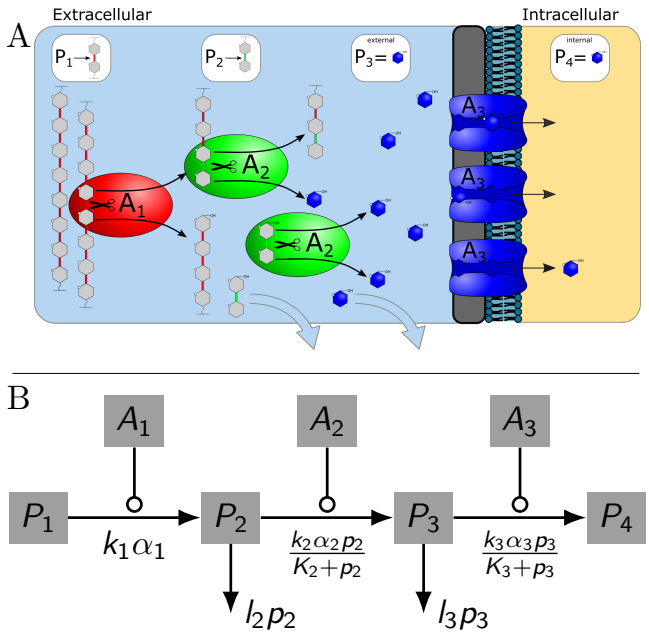

Figure 1. (A) Amylose degradation by *A. niger*. The α-amylase (A1) dissects amylose by removing a bond between units of glucose (P1). This results in one extra molecule having a bond connected to a non-reducing end (P2), which can now be dissected by the enzymes α-glucosidase and glucoamylase (A2) yielding external glucose monomers (P3). These monomers are transported (through A3) into the hypha (P4). Oligosaccharides (represented by P2) and external glucose are lost at a fixed rate through diffusion or uptake by rival organisms. (B) Mathematical model. A sequence of products P_i (concentrations p_i) undergoing reactions catalysed by A_i (concentrations α_i). P_1 is assumed to be present in high concentration so that the reaction rate towards P_2, $k_1\alpha_1$, does not depend on p_1. Other reactions are according to Michaelis-Menten [21] kinetics: $\frac{k_i\alpha_i p_i}{K_i+p_i}$. For facilitated transport this form holds under the assumption that the concentration p_4 is (kept) low, so backward transport is negligible [22]. For glucose uptake by *A. niger* the Michaelis-Menten kinetics was confirmed experimentally [23]. Intermediates P_2 and P_3 undergo a loss of l_2p_2 and l_3p_3, respectively.

an Arduino Nano V3 via I2C. A SSD1306 0.96 inch oled IIC Serial White OLED Display Module (128 X 64 pixels) was also connected through I2C to output the sensor readings every 5 seconds. A bespoke PCB was designed in Fritzing to connect all hardware by soldering. The device was powered through the ISP header pins Vcc and Gnd via a 3 AA cell battery holder. The Arduino code to drive the logger and the PCB design are available on request.

The fungal biomass was quantified by harvesting the sandwich colony. To this end, the sandwich colony was placed in a new petri dish and the top membrane was removed. The colony was flipped over and the second membrane was removed. The mycelium was subsequently dried for 5 days at 60 °C and the resulting dry weight of the biomass was weighed.

(d) Statistics

Differences in metabolic activity between N402 and N402Δ*hexA* were assessed by dividing the absolute difference in carbon dioxide levels over 3 minutes (ppm) by the total biomass (mg) of each colony. The assumption of normality was tested for each data set using a Levene's test. The p-value and confidence interval were tested using a Two Sample t-test. The power was tested using Vanderbilt PS: Power and Sample Size Calculation version 3.1.6, October 2018 (Dupont & Plummer, n.d.).

3. Results

(a) Model: heterogeneous is more efficient

We use a mathematical model (see section 2(a)) to study how concentrating catalysts at hyphae influences the efficiency of starch degradation. For each distribution of the catalyst concentrations α_1 (α-amylases), α_2 (glucoamylases combined with α-glucosidases) and α_3 (glucose transporters) we determined the speed at which hyphae absorb glucose - the harvest rate - in equilibrium. For the sake of simplicity, we restrict our attention to two otherwise identical hyphae, and vary the distribution of the catalysts under the constraint that the total amount of each catalyst remains constant.

First suppose that at both hyphae $\alpha_i = 1$ for each catalyst so that both hyphae harvest the same amount of glucose. This is the homogeneous benchmark (Fig. 2; orange scenario). Now, if instead the first catalyst is concentrated at one hypha, the other hypha stops harvesting. In case the other catalysts are evenly split, this results in a lower average harvest rate than the benchmark (Fig. 2; red scenario). With all three catalysts concentrated at one hypha, the amylolytic process is more efficient than the benchmark (Fig. 2; blue scenario). Conceptually, only concentrating the first catalyst leads to congestion at subsequent steps and relatively high loss terms, while concentrating all catalysts yields high throughput and relatively low losses.

The intermediate scenario is where two out of three catalysts are concentrated at one hypha (Fig. 2; green scenario). Concentrating the second catalyst α_2 results in less congestion at the second step, but partially at the expense of more congestion at the third step. In Fig. 2 the harvest rate is larger than that of the benchmark. By changing the reaction constant of the first reaction k_1 from the default value $k_1 = 1$ to $k_1 = 10$, leading to more congestion, concentrating two catalysts can also result in a harvest rate that is lower than the benchmark (electronic supplementary material, Fig. S5).

The graphs in Fig. 2 help explain these results. The red curve has a decreasing slope, so concentrating one catalyst leads to a diminishing return of investment. So there is no incentive to concentrate only the first catalyst. The blue curve has an increasing slope, so concentrating all catalysts leads to an increasing return of investment. This economy of scale is an incentive to concentrate all catalyst at one hypha. The green curve is sigmoidal, so concentrating part of the catalysts can either lead to a diminishing or increasing return. Thus, the model shows that heterogeneity permits a higher glucose harvest rate.

Importantly, the majority of our results do not depend on the choice of parameter values: within our model framework concentrating one catalyst always results in a diminishing return of investment and increasing all catalyst concentrations always results in an increasing return of investment. Increasing multiple but not all catalyst concentrations always results in a sigmoidal curve. Only the location of the switch from increasing to diminishing return depends on parameter values. The general picture is sketched in Fig. 3. Sensitivity analysis, generalisation and mathematical proofs can be found in the electronic supplementary material.

(b) Experimental validation

Both the amylolytic regulatory gene *amyR* and the amylolytic enzymes encoding genes *aamA* (α-amylase, α_1) and *glaA* (glucoamylase, α_2), are heterogeneously co-expressed in the wild type [11,13]. The absence of Woronin bodies results in the elimination of septal plugging and thereby the loss of heterogeneity of amylolytic gene expression in the *hexA* mutant [16,20]. We used these strains to test the outcome of our model: that concentrating catalysts permits a higher glucose harvest rates than homogeneously distributing all catalysts.

To this end, sandwich colonies of the *A. niger* strains N402 (wild type) and N402Δ*hexA* (mutant) were grown for 5 days on 200 mM xylose, after which they were transferred for 8 hours to MM agar plates supplemented with 2% starch to induce amylolytic activity [25]. After 8 hours starch was still present underneath the colonies, while most starch was degraded after 24

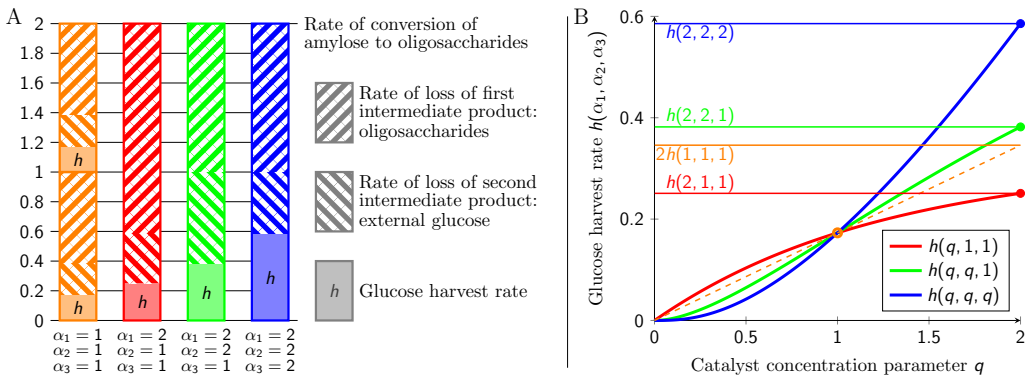

Figure 2. The process of amylose degradation depending on how catalyst is split over two hyphae, keeping the average catalyst concentrations $\alpha_1, \alpha_2, \alpha_3$ equal to 1. (A) The total rate of conversion of amylose, the first step in the three-step process, is the same in all scenarios and equals 2. Intermediates (oligosaccharides and external glucose) are lost due to diffusion or uptake by rival organisms, resulting in a lower glucose harvest rate, which is dependent on the scenario. Orange scenario (benchmark): fifty-fifty distribution of all catalysts, so that $\alpha_1 = \alpha_2 = \alpha_3 = 1$ in both hyphae, resulting in a harvest rate of $h(1,1,1) \approx 0.17$ twice. Red: only $\alpha_1 = 2$ is concentrated at one hypha; α_2 and α_3 are evenly split. Harvest is restricted to one hypha with rate $h(2,1,1) \approx 0.25 < 2h(1,1,1)$, so smaller than the benchmark. Green: additionally α_2 is concentrated at one hypha; α_3 remains evenly split ($\alpha_3 = 1$). Harvest is restricted to one hypha with rate $h(2,2,1) \approx 0.38 > 2h(1,1,1)$, so larger than the benchmark. Compared to the red scenario, concentrating α_2 results in a drop of the loss of the first intermediate product, but the loss of the second intermediate increases. Blue: also α_3 is concentrated at one hypha. Harvest is restricted to one hypha with rate $h(2,2,2) \approx 0.59$ which outperforms all other scenarios. (B) Harvest rate as a function of catalyst concentrations for the three heterogeneous scenarios. All curves pass through the benchmark (orange circle) at $q = 1$. Since the red curve has a decreasing slope, concentrating only α_1 yields a diminishing return of investment. The blue curve has an increasing slope, so there is an increasing return of investment: economy of scale. The green curve is sigmoidal and because here at $q = 1$ the slope is increasing, it also has an increasing return of investment. Explicit formulas for the curves can be found in the electronic supplementary material.

hours (electronic supplementary material, Fig. S7). Thus, the metabolic activity of both strains was determined after 8 hours by measuring the carbon dioxide production over 3 minutes, corrected for biomass.

A significant difference in metabolic activity between the wild type and the mutant strain was observed. On average, the metabolic activity (CO_2 production/mg biomass) was 48% higher ($p = 0.043$, $\mathrm{power} = 1.00$) in the heterogeneous wild type in respect to the mutant strain. This implies that also the glucose harvest rate of the wild type is higher than that of the mutant strain. But there was no apparent distinction between the amount of remaining amylose (starch) for the two strains after 8 and 24 hours (electronic supplementary material, Fig. S7). Of note, lugol can only bind the helix structure of starch, but not its degradation products, that lack this structure. The difference in harvest rate is thus not due to a difference in conversion rate from amylose to oligosaccharides, but must be due to efficiency of heterogeneity in subsequent conversion steps, which is in agreement with the model (Fig. 2).

In contrast, the average biomass of N402 and N402Δ*hexA*, 69.31 and $68.01\mathrm{mg}$, respectively, did not show a significant difference ($p = 0.58$, $\mathrm{power} = 0.07$). Most of the growth occurs during the preliminary 5 days on xylose. Since uptake of xylose is a one-step process, here cellular heterogeneity is not predicted to have an effect according to our model, which explains why the average biomass is not significantly different. Thus, the biological experiments support the model.

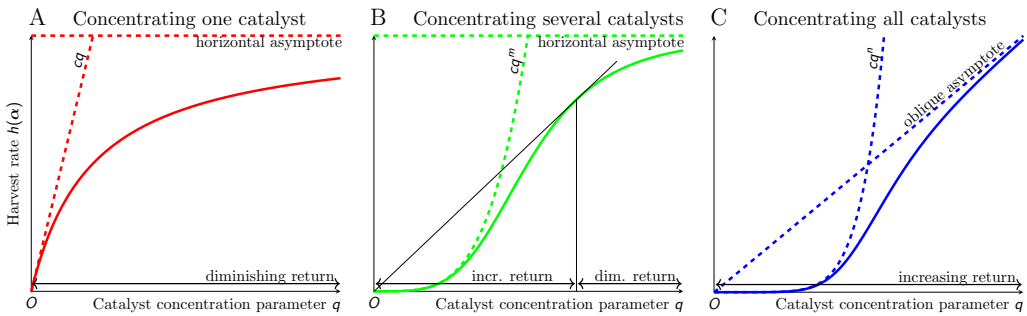

Figure 3. General picture of the dependence of the harvest rate on the catalyst concentration parameter q, depending on the number of catalyst concentrations that depend on q. The limiting behavior for low and high q is determined by Corollaries 3 and 4 of the electronic supplementary material. (A) Only one catalyst concentration depends on q. In this case, there is always a diminishing return of investment (electronic supplementary material, Corollary 1). (B) Multiple m (but not all n) catalyst concentrations depend on q. The harvest rate is a sigmoidal function so that concentrating multiple (but not all) catalysts can both lead to an increasing and diminishing return of investment (electronic supplementary material, Corollary 5). See supplementary material Fig. S5 and S6 where this is worked out for the amylolytic model. (C) All n catalyst concentrations depend on q. In this case, there is always an increasing return of investment (electronic supplementary material, Corollary 2).

(c) Model: self-organisation enables heterogeneity

In the previous sections we have shown that starch degradation by *A. niger* is more efficient if the hyphae specialise into subpopulations of highly active and lowly active hyphae. We now sketch how, with minimal adaptation of the model, this heterogeneity can be realized through self-organisation.

It is known that the production of amylolytic enzymes (with concentration α_1 and α_2) is induced by (iso)maltose (represented by concentration p_2) by upregulation through AmyR [7]. Since increasing α_1 results in a higher production of p_2, this may yield a positive feedback.

The induction by (iso)maltose depends on the external concentration of maltose and the amount of maltose transporters. Maltose itself leads to increased expression of maltose transporters ([26] and reviewed by [27]). Moreover, α-gluscosidases in *Aspergillus* catalyse the formation of isomaltose [25]. For these reasons, the strength of the induction is likely a non-linear function of external maltose concentration p_2. We postulate that α_1 and α_2 both on p_2 through a function that resembles a sigmoid (also found in [28]). For the sake of simplicity we choose $\alpha_1 = \alpha_2 = \min(c{p_2}^2, 2)$. This means that they depend quadratically on p_2 but cannot increase beyond the value 2.

The coefficient c controls the strength of the upregulation. Provided c is sufficiently large, this results in bi-stability of highly and lowly active hyphae. In Fig. 4, three bi-stable configurations are depicted. Each hypha can only reside in one of the two stable equilibria ($p_2 = \alpha_1 = \alpha_2 = 0$ or $p_2 = 1$ and $\alpha_1 = \alpha_2 = 2$) corresponding to low or high activity.

The strength of the upregulation c determines how the basins of attraction (bounded by the unstable equilibrium) are positioned. A larger basin of attraction generally leads to a larger proportion of hyphae converging to the corresponding equilibrium. By modulating the percentage of highly active hyphae the glucose concentration inside the mycelium may be managed. Too many active hyphae would result in a high internal glucose concentration, which induces the retention of CreA to the nucleus, which in turn inhibits the production of amylolytic enzymes [29]. The strength of the upregulation c thus decreases and so would the percentage of highly active hyphae, reducing the influx of glucose. This way, the hyphae would dynamically self-organize into a lowly and highly active subpopulation. Varying proportions between lowly and highly active hyphae of *A. niger* have been observed, depending on the conditions [11].

It is currently not known whether the concentration of glucose transporters α_3 in the hyphal cell membrane also depends on p_2 like α_1 and α_2. For bi-stability of the system this is irrelevant, because α_3 does not influence p_2. However, it would improve the efficiency, namely from the green scenario in Fig. 2 to the blue scenario. The dependence of α_3 on p_2 could also be indirect, e.g. through dependence of α_3 on the external glucose concentration p_3 [30]. Either way, we conclude that a minimal model adjustment enables heterogeneity through self-organisation, and more efficient starch degradation.

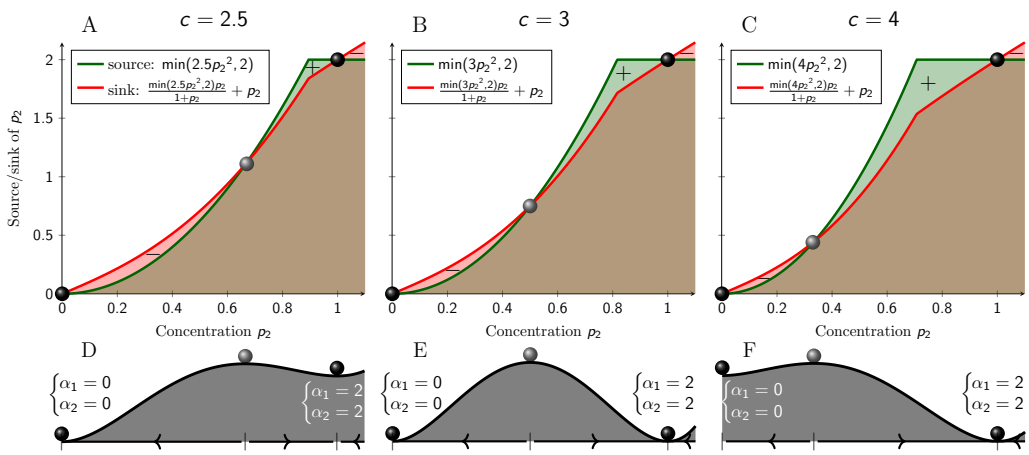

Figure 4. (A-C) Source term (green curve) and sum of two sink terms (red) of p_2 (related to oligosaccharides) as a function of p_2 itself, with upregulation $\alpha_1 = \alpha_2 = \min(cp_2{}^2, 2)$ with varying strength: $c = 2.5$ (A), $c = 3$ (B) and $c = 4$ (C). Equilibria when source and sink terms are equal are depicted by balls, which are either stable (black) or unstable (gray). (D-F) The coefficient c modulates the location of the unstable equilibrium in the middle and thus the basins of attraction of the two stable equilibria, where either $\alpha_1 = \alpha_2 = 0$ (on the left) or $\alpha_1 = \alpha_2 = 2$ (on the right), for $c = 2.5$ (D), $c = 3$ (E) and $c = 4$ (F).

4. Discussion

In this study we showed that self-organisation optimizes multi-step processes. Specifically, we showed by both modeling and biological experiments that hyphal heterogeneity in *A. niger*, observed in [11], enhances the efficiency of starch degradation. For simplicity, we restricted ourselves to the linear amylose component of starch in the model but it is extendable to amylopectin by including a preliminary reaction step. Within our general multi-step mathematical framework we prove that concentrating one catalyst is never beneficial. Only if multiple (preferably all) catalysts are concentrated this permits a higher overall harvest rate. Master controller genes or transcription factors such as AmyR affecting multiple steps at once are thus not only convenient but also necessary for evolution towards more efficient heterogeneous transcription.

Our model analysis assumes that the glucose harvest rate is in equilibrium. After exposure of *A. niger* to starch and induction of amylolytic enzymes, hyphae with lower catalyst concentrations need longer to reach their equilibrium harvest rate, because the concentration of intermediates in this case builds up relatively slowly. Part of the difference in metabolic activity observed in our experiment may be due to the *hexA* mutant not having reached its equilibrium harvest rate, but this only underscores the efficiency of heterogeneity.

Our results relate to the concept of *dissipative structure* coined by Ilya Prigogine (Nobel prize in chemistry, 1977). Here, "dissipative" refers to a thermodynamically open system, which need not evolve to equilibrium. Because there is a continuous supply of amylose, the amylolytic model is

also open and the differences in activity of the hyphae is linked to dissipative structure. In [31] it was stated that "biological structures can only originate (...) and be maintained by a continuous supply of energy". Here it was also contemplated that "In the inhomogeneous state (...) the overall reaction rate is increased". In this article we indeed have shown how, within our multi-step model framework, heterogeneity permits a higher over-all reaction rate. This is at odds with the previous perception that heterogeneity leads to sub-optimal production in e.g. bioreactors, since not all micro colonies participate in production [18,32]. Instead, we find that the maximum production level can only be attained through heterogeneity. Thus, contrary to what the name might suggest, dissipative structure is economic.

Because of the generality of our model framework and natural selection of efficient processes, we expect that it is applicable in other kingdoms of life at possibly other length scales. Necessary and sufficient conditions within our framework are 1) a multi-step process where the reaction speed of multiple steps can be influenced, 2) sufficient separation to allow differentiation (in case of amylolysis by septal plugging impeding cytoplasmic mixing) and 3) some loss of intermediate products. In amylolysis, the intermediates are external glucose and oligosaccharides. While the intermediates have not been transported yet into the hyphae, there is loss due to diffusion or uptake by rival organisms. With the three conditions in mind, we end by highlighting similarities, applicability and limitations of the model framework to four more cases in a broad range of contexts (Fig. 5B-E).

Starting close to home, next to starch, *Aspergillus* can degrade many more complex substrates, and this degradation is generally mediated by specific transcriptional regulators such as AmyR. For example, XlnR regulates the expression of xylanolytic enzymes [33], which break down xylan sequentially (reviewed in [34]), see Fig. 5B. Xylooligosaccharides trigger the expression of XlnR [35], transcription is again down-regulated by CreA [36]. As degradation of xylan proceeds in multiple steps, concentrating enzyme production in part of the hyphae again permits a more efficient substrate degradation. Expression of xylanolytic genes is known to be heterogeneous: the production of *faeA* and *aguA* is again separated in two distinct hyphal populations [13]. The corresponding enzymes remove side chains, which could be included in the model as a preliminary step. Whether the enzymes that degrade the main chain are also heterogeneously expressed remains to be investigated.

Secondly, the lac operon of *E. coli* [37] regulates two steps in the digestion and uptake of lactose (Fig. 5C). Specifically, both the membrane protein that enables transport of lactose into the cell and the enzyme that cleaves lactose are induced by (allo)lactose (condition (1)). Since the intermediate - internal lactose - is intracellular, it cannot be lost through diffusion or uptake by rival organisms. Loss may be interpreted more broadly by acknowledging that maintaining an intracellular metabolite concentration incurs a homeostatic cost (condition 3). The overall homeostatic cost at the population level would then be lower if cleavage of lactose is performed in only part of the bacteria (keeping overall catalyst concentration constant), while the harvest rate remains the same, thereby potentially increasing overall efficiency. On the population level, there is sufficient separation for heterogeneity (condition (2)). Leakage [39] of glucose or galactose could be part of a division of labour; specialisation by bacteria has been observed in biofilms [40]. The lac operon was found to be bi-stable for induction by artificial inducer but less likely so for the natural inducer (allo)lactose [41–43].

In the previously discussed cases, sufficient separation for differentiation (condition (2)) was ensured because hyphae or entire cells acted as compartments. On a smaller scale, subcellular compartmentalisation facilitates metabolite or substrate channelling: the transfer of intermediates from one enzyme to the next [44–46]. A prominent example of channelling is glycolysis (reviewed in [47]). Here, ten enzymes catalyse the conversion of glucose into pyruvate (condition (1)), see Fig. 5D. Intermediates of glycolysis are involved in side reactions, which are then lost from the glycolytic pathway (condition (3)). Channelling is a way to regulate the metabolic flux network and improve the efficiency of the channelled pathway by lowering the chance that intermediates are lost from that pathway [48–50] or to protect homeostasis by keeping the

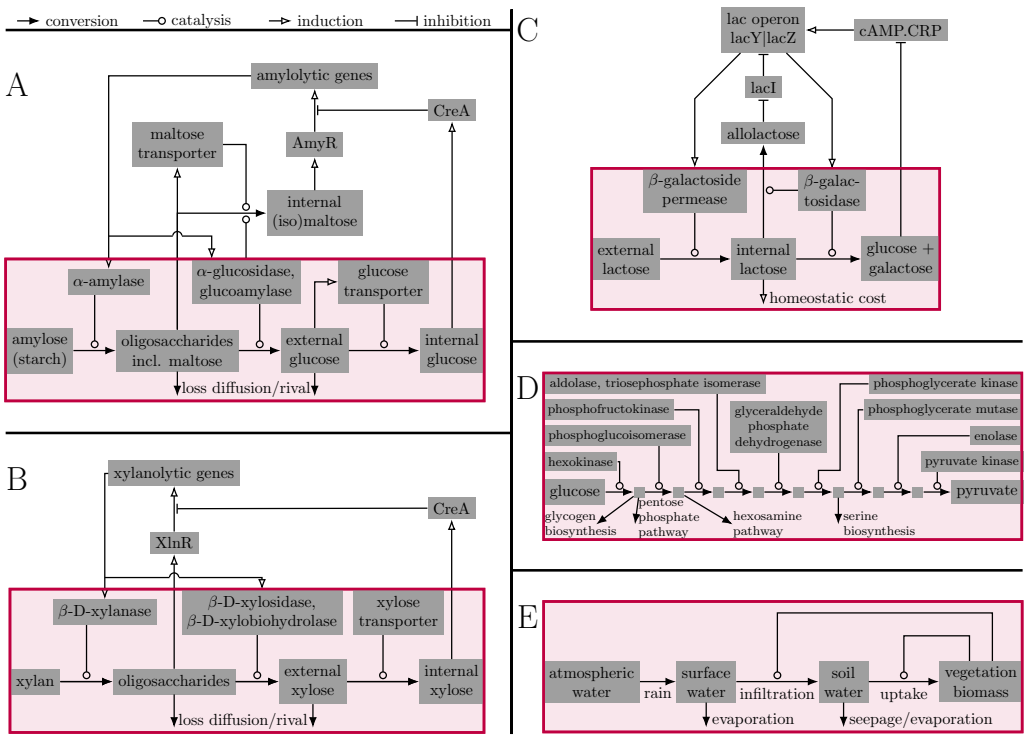

Figure 5. Similarity between A) amylolysis and B) xylanolysis by *A. niger*, C) uptake and digestion of lactose by *E. coli*, D) glycolysis and E) water harvesting by dryland vegetation. A) Amylolytic pathway. Within the box the minimal model of catalysed degradation of starch, with regulatory network outside the box. (Iso)maltose promotes transcription of amylolytic genes through upregulation of AmyR [7], resulting in production of amylolytic genes. Maltose leads to increased expression of maltose transporters ([26] and reviewed by [27]), and α-gluscosidases in *Aspergillus* catalyse the formation of isomaltose [25]. The external glucose concentration influences the presence of glucose transporters [30]. The end product, internal glucose, inhibits the production of enzymes through the catabolic respressor CreA [29]. B) Xynalolytic pathway. The minimal model (within red box) and regulatory network is very similar to that of amylolysis. XlnR regulates the expression of xylanolytic enzymes [33], which break down xylan sequentially (reviewed in [34]). Xylooligosaccharides trigger the expression of XlnR [35], transcription is again down-regulated by CreA [36]. C) Lactolytic pathway. The red box shows a minimal model. Both the membrane protein that enables transport of lactose into the cell and the enzyme that cleaves lactose are induced by the intermediate (allo)lactose [37], which is similar to A) and B), but this time through inhibition of an inhibitor. Also, glucose again inhibits the production of the catalysts: here glucose represses cAMP, which after binding to its receptor protein (CRP) would promote the production of catalyst [38]. Since the intermediate - internal lactose - is intracellular, it may not be lost through diffusion or uptake by rival organisms. Loss may be interpreted more broadly by acknowledging that maintaining an intracellular metabolite concentration induces a homeostatic cost. D) Glycolytic pathway. Only the minimal model without regulatory network is shown. Ten enzymes together sequentially convert glucose into pyruvate. The reactions are again intracellular, loss of intermediates may in this case be interpreted by other pathways competing for intermediates. E) Harvesting of rain water by dryland vegetation. Here the end product vegetation itself acts as a catalyst, increasing both the infiltration and the uptake rate. This is opposite to A-C, where end products inhibit the production of catalysts (to prevent overproduction). In the dryland context there is no regulatory network.

concentration of intermediates low [51]. The end product of glycolysis, pyruvate, is subjected to oxidative decarboxylation by the pyruvate dehydrogenase complex of three enzymes, which is also a form of substrate channelling. The resulting acetyl-CoA enters the Krebs cycle, with corresponding enzymes concentrated in mitochondria, another from of substrate channelling by subcellular localization. The entire chain from glycolysis up to and including the Krebs cycle

could function as one partially channelled pathway: if the respiration rate increases, glycolytic enzymes dynamically associate to the outer surface of mitochondria [52]. Other examples of dynamic substrate channelling are hypoxic stress leading to compartmentalisation of glycolysis enzymes [53] and the level of purine influencing the association and dissociation of enzyme clusters in purine biosynthesis [54].

As a fourth and final case, we apply our model framework to vegetation patterns in drylands. These patterns were first reported in 1950 based on air photography [55]. With distances of tens to hundreds of meters between patches of vegetation, interspersed with bare soil, this heterogeneity operates on an entirely different scale. An explanation for the emergence of self-organisation is that the water infiltration rate is higher within vegetated patches [56,57], so there is a local facilitation effect, similar to biofilms. In a second step, infiltrated water is taken up by the vegetation. The reaction speed of both steps, infiltration and uptake, is increased by vegetation (condition (1), Fig. 5E). Vegetation can separate into patches over generations (condition (2)). And if water is not taken up, it evaporates or seeps away (condition (3)). Models for dryland vegetation patterns that incorporate the infiltration feedback, e.g. [58,59], fit our model framework. Accordingly, clustered vegetation harvests water more efficiently than homogenously distributed vegetation, thereby improving resilience against drought (reviewed by [60]).

Dryland vegetation forms a regular Turing pattern [61,62]. A topic of ongoing research is whether the population of highly active hyphae in *A. niger* also forms a regular pattern. We expect that hyphae neighbouring highly active hyphae may also have a tendency to become highly active, resulting in clumps of hyphae that jointly break down the substrate. The size of these clumps would be determined by the spreading speed of inducing oligosaccharides like maltose in relation to that of glucose - which spreads faster and leads to catabolic respression through CreA - and the need for glucose. Around these clumps there may be hyphae that only express increased concentration of glucose transporters, harvesting external glucose without taking part in the enzymatic degradation. The resulting high internal glucose concentration would oppose the production of amylolytic enzymes in these hyphae. The spacing between clumps arguably depends on the mobility of glucose. If glucose moves relatively fast (e.g. via cytoplasmic streaming [63]), clumps of highly active hyphae may lie further apart from each other, since lowly active hyphae need not be in the direct vicinity of highly active hyphae to acquire sufficient glucose for homeostasis. As substrate is locally depleted, the positions of active clumps may change dynamically.

Dryland vegetation pattern formation occurs without extensive regulatory network (Fig. 5E), so the patterns are truely *self*-organised. For the metabolism of *Aspergillus*, self-organisation is facilitated by a regulatory network, so this is a type of *organised self-organisation*. In Fig. 5D, no regularity network of the glucolytic pathway is shown but it easily outcompetes the other examples in terms of complexity. Here, self-organisation may still play a role in self-assembly of compartmentalisation [47,64], but the entire process seems to be more on the organised rather than self-organised side.

Life has evolved to carry out complex processes efficiently. By organisation and specialisation, the overall efficiency can be improved. We have shown this also applies to self-organisation in the context of multi-step processes, so higher yield is possible with minimal control. This improves fitness in situations where full control is not possible, e.g. if part of the process is extracellular. An additional benefit is that self-organised patterns can more easily adapt to changing conditions, allowing for greater flexibility as compared to more rigid structures in life.

The interplay between self-organisation and natural selection (e.g. [65–71]) remains an intriguing topic to study. Our work also has practical implications. For instance, allowing for heterogeneity in bio-reactors may result in higher overall production. On another level, forcing vegetation to grow in between patches runs the risk of loosing biomass altogether. Fields ranging from biotechnology to ecosystem management may thus benefit from facilitating self-organisation.

Acknowledgements. The initial phase of this research was supported by NWO TTW grant 'Traffic control' [15493]. R.B. was supported by NWO TTW Vidi grant 'Feed me' [18920]. The funders were not involved in study design, in the analysis, the writing of the article or the decision to submit for publication.

References

1. Riquelme M, Roberson RW, Sánchez-León E. 2016 pp. 47–66. In *3 Hyphal Tip Growth in Filamentous Fungi*, pp. 47–66. Cham: Springer International Publishing. (10.1007/978-3-319-25844-7$_3$)
2. Steinberg G, Peñalva MA, Riquelme M, Wösten HA, Harris SD. 2017 Cell Biology of Hyphal Growth. *Microbiol Spectr* **5**.
3. Wang BT, Hu S, Yu XY, Jin L, Zhu YJ, Jin FJ. 2020 Studies of Cellulose and Starch Utilization and the Regulatory Mechanisms of Related Enzymes in Fungi. *Polymers* **12**. (10.3390/polym12030530)
4. Zeeman SC, Kossmann J, Smith AM. 2010 Starch: its metabolism, evolution, and biotechnological modification in plants. *Annu Rev Plant Biol* **61**, 209–234.
5. Coutinho P, Henrissat B. 1999 pp. 3–12. In *Carbohydrate-active enzymes: an integrated database approach*, pp. 3–12. Cambridge: The Royal Society of Chemistry.
6. Yuan XL, van der Kaaij RM, van den Hondel CAMJJ, Punt PJ, van der Maarel MJEC, Dijkhuizen L, Ram AFJ. 2008 Aspergillus niger genome-wide analysis reveals a large number of novel alpha-glucan acting enzymes with unexpected expression profiles. *Molecular Genetics and Genomics* **279**, 545–561. (10.1007/s00438-008-0332-7)
7. Murakoshi Y, Makita T, Kato M, Kobayashi T. 2012 Comparison and characterization of α-amylase inducers in Aspergillus nidulans based on nuclear localization of AmyR. *Applied microbiology and biotechnology* **94**, 1629–1635.
8. Tani S, Itoh T, Kato M, Kobayashi T, Tsukagoshi N. 2001 In vivo and in vitro analyses of the AmyR binding site of the Aspergillus nidulans agdA promoter; requirement of the CGG direct repeat for induction and high affinity binding of AmyR. *Biosci Biotechnol Biochem* **65**, 1568–1574.
9. Quistgaard EM, Löw C, Guettou F, Nordlund P. 2016 Understanding transport by the major facilitator superfamily (MFS): structures pave the way. *Nature Reviews Molecular Cell Biology* **17**, 123–132. (10.1038/nrm.2015.25)
10. Wösten HA, Moukha SM, Sietsma JH, Wessels JG. 1991 Localization of growth and secretion of proteins in Aspergillus niger. *J Gen Microbiol* **137**, 2017–2023.
11. Vinck A, Terlou M, Pestman WR, Martens EP, Ram AF, van den Hondel CAMJJ, Wösten HAB. 2005 Hyphal differentiation in the exploring mycelium of Aspergillus niger. *Molecular Microbiology* **58**, 693–699. (https://doi.org/10.1111/j.1365-2958.2005.04869.x)
12. Levin AM, de Vries RP, Conesa A, de Bekker C, Talon M, Menke HH, van Peij NNME, Wösten HAB. 2007 Spatial Differentiation in the Vegetative Mycelium of Aspergillus niger. *Eukaryotic Cell* **6**, 2311–2322. (10.1128/ec.00244-07)
13. Vinck A, de Bekker C, Ossin A, Ohm RA, de Vries RP, Wösten HAB. 2011 Heterogenic expression of genes encoding secreted proteins at the periphery of Aspergillus niger colonies. *Environmental Microbiology* **13**, 216–225. (https://doi.org/10.1111/j.1462-2920.2010.02322.x)
14. Jedd G, Chua NH. 2000 A new self-assembled peroxisomal vesicle required for efficient resealing of the plasma membrane. *Nature Cell Biology* **2**, 226–231. (10.1038/35008652)
15. Tenney K, Hunt I, Sweigard J, Pounder JI, McClain C, Bowman EJ, Bowman BJ. 2000 Hex-1, a gene unique to filamentous fungi, encodes the major protein of the Woronin body and functions as a plug for septal pores. *Fungal Genet Biol* **31**, 205–217.
16. Bleichrodt RJ, Van Veluw J, Recter B, Maruyama Ji, Kitamoto K, Wosten H. 2012 Hyphal heterogeneity in Aspergillus oryzae is the result of dynamic closure of septa by Woronin bodies. *Molecular microbiology* **86**. (10.1111/mmi.12077)
17. Bleichrodt RJ, Hulsman M, Wösten HAB, Reinders MJT. 2015 Switching from a Unicellular to Multicellular Organization in an Aspergillus niger Hypha. *mBio* **6**, 10.1128/mbio.00111–15. (10.1128/mbio.00111-15)
18. de Bekker C, van Veluw G, Vinck A, Wiebenga L, Wösten H. 2011 Heterogeneity of Aspergillus niger Microcolonies in Liquid Shaken Cultures. *Applied and Environmental Microbiology* **77**, 1263–1267. (10.1128/AEM.02134-10)

19. Hewitt SK, Foster DS, Dyer PS, Avery SV. 2016 Phenotypic heterogeneity in fungi: Importance and methodology. *Fungal Biology Reviews* **30**, 176–184. (https://doi.org/10.1016/j.fbr.2016.09.002)
20. Tegelaar M, Bleichrodt RJ, Nitsche B, Ram AFJ, Wösten HAB. 2020 Subpopulations of hyphae secrete proteins or resist heat stress in Aspergillus oryzae colonies. *Environmental Microbiology* **22**, 447–455. (https://doi.org/10.1111/1462-2920.14863)
21. Michaelis L, Menten ML. 1913 Die Kinetik der Invertinwirkung. *Biochemische Zeitschrift* **49**, 333 – 369.
22. Widdas W. 1952 Inability of diffusion to account for placental glucose transfer in the sheep and consideration of the kinetics of a possible carrier transfer. *The Journal of physiology* **118**, 23.
23. Lameiras F, Ras C, ten Pierick A, Heijnen JJ, van Gulik WM. 2018 Stoichiometry and kinetics of single and mixed substrate uptake in Aspergillus niger. *Bioprocess and Biosystems Engineering* **41**, 157–170. (10.1007/s00449-017-1854-3)
24. de Vries RP, Burgers K, van de Vondervoort PJI, Frisvad JC, Samson RA, Visser J. 2004 A New Black Aspergillus Species, A. vadensis, Is a Promising Host for Homologous and Heterologous Protein Production. *Applied and Environmental Microbiology* **70**, 3954–3959. (10.1128/AEM.70.7.3954-3959.2004)
25. Kato N, Murakoshi Y, Kato M, Kobayashi T, Tsukagoshi N. 2002 Isomaltose formed by α-glucosidases triggers amylase induction in Aspergillus nidulans. *Current Genetics* **42**, 43–50. (10.1007/s00294-002-0325-8)
26. Suzuki K, Tanaka M, Konno Y, Ichikawa T, Ichinose S, Hasegawa-Shiro S, Shintani T, Gomi K. 2015 Distinct mechanism of activation of two transcription factors, AmyR and MalR, involved in amylolytic enzyme production in Aspergillus oryzae. *Applied microbiology and biotechnology* **99**, 1805–1815.
27. Tanaka M, Gomi K. 2021 Induction and Repression of Hydrolase Genes in Aspergillus oryzae. *Front Microbiol* **12**, 677603.
28. Zuin J, Roth G, Zhan Y, Cramard J, Redolfi J, Piskadlo E, Mach P, Kryzhanovska M, Tihanyi G, Kohler H, Eder M, Leemans C, van Steensel B, Meister P, Smallwood S, Giorgetti L. 2022 Nonlinear control of transcription through enhancer–promoter interactions. *Nature* **604**, 571–577. (10.1038/s41586-022-04570-y)
29. Tanaka M, Ichinose S, Shintani T, Gomi K. 2018 Nuclear export-dependent degradation of the carbon catabolite repressor CreA is regulated by a region located near the C-terminus in Aspergillus oryzae. *Mol Microbiol* **110**, 176–190.
30. Torres NV, Riol-Cimas JM, Wolschek M, Kubicek CP. 1996 Glucose transport by Aspergillus niger: the low-affinity carrier is only formed during growth on high glucose concentrations. *Applied Microbiology and Biotechnology* **44**, 790–794. (10.1007/BF00178620)
31. Prigogine I, Nicolis G. 1967 On Symmetry-Breaking Instabilities in Dissipative Systems. *The Journal of Chemical Physics* **46**, 3542–3550. (10.1063/1.1841255)
32. Wösten HAB, van Veluw GJ, de Bekker C, Krijgsheld P. 2013 Heterogeneity in the mycelium: implications for the use of fungi as cell factories. *Biotechnology Letters* **35**, 1155–1164. (10.1007/s10529-013-1210-x)
33. van Peij NN, Gielkens MM, de Vries RP, Visser J, de Graaff LH. 1998 The transcriptional activator XlnR regulates both xylanolytic and endoglucanase gene expression in Aspergillus niger. *Appl Environ Microbiol* **64**, 3615–3619.
34. Li X, Dilokpimol A, Kabel M, de Vries R. 2022 Fungal xylanolytic enzymes: Diversity and applications. *Bioresource Technology* **344**, 126290. (https://doi.org/10.1016/j.biortech.2021.126290)
35. Weili W, Dai L, Zhang H, Zhang L, Wang L. 2018 A Highly Efficient Xylan-Utilization System in Aspergillus niger An76: A Functional-Proteomics Study. *Frontiers in Microbiology* **9**. (10.3389/fmicb.2018.00430)
36. de Vries R, Visser J, de Graaff L. 1999 CreA modulates the XlnR-induced expression on xylose of Aspergillus niger genes involved in xylan degradation. *Research in Microbiology* **150**, 281–285. (https://doi.org/10.1016/S0923-2508(99)80053-9)
37. Jacob F, Monod J. 1961 Genetic regulatory mechanisms in the synthesis of proteins. *Journal of Molecular Biology* **3**, 318–356. (https://doi.org/10.1016/S0022-2836(61)80072-7)
38. Busby S, Ebright RH. 1999 Transcription activation by catabolite activator protein (CAP). *Journal of Molecular Biology* **293**, 199–213. (https://doi.org/10.1006/jmbi.1999.3161)
39. McKinlay JB. 2023 Are bacteria leaky? Mechanisms of metabolite externalization in bacterial cross-feeding. *Annu. Rev. Microbiol.* **77**, 277–297.

40. Dragoš A, Kiesewalter H, Martin M, Hsu CY, Hartmann R, Wechsler T, Eriksen C, Brix S, Drescher K, Stanley-Wall N, Kümmerli R, Kovács ÁT. 2018 Division of Labor during Biofilm Matrix Production. *Curr Biol* **28**, 1903–1913.e5.
41. Ozbudak EM, Thattai M, Lim HN, Shraiman BI, van Oudenaarden A. 2004 Multistability in the lactose utilization network of Escherichia coli. *Nature* **427**, 737–740. (10.1038/nature02298)
42. van Hoek M, Hogeweg P. 2006 In Silico Evolved lac Operons Exhibit Bistability for Artificial Inducers, but Not for Lactose. *Biophysical Journal* **91**, 2833–2843. (https://doi.org/10.1529/biophysj.105.077420)
43. Dreisigmeyer DW, Stajic J, Nemenman I, Hlavacek WS, Wall ME. 2008 Determinants of bistability in induction of the Escherichia coli lac operon. *IET Syst Biol* **2**, 293–303.
44. Srere P. 1987 Complexes of sequential metabolic enzymes. *Annual Review of Biochemistry* **56**, 89–124. (https://doi.org/10.1146/annurev.bi.56.070187.000513)
45. Ovádi J, Saks V. 2004 On the origin of intracellular compartmentation and organized metabolic systems. *Mol Cell Biochem* **256-257**, 5–12.
46. Lee H, DeLoache W, Dueber J. 2012 Spatial organization of enzymes for metabolic engineering. *Metabolic Engineering* **14**, 242–251. Synthetic Biology: New Methodologies and Applications for Metabolic Engineering (https://doi.org/10.1016/j.ymben.2011.09.003)
47. Fuller G, Kim J. 2021 Compartmentalization and metabolic regulation of glycolysis. *J Cell Sci* **134**.
48. Castellana M, Wilson M, Xu Y, Joshi P, Cristea I, Rabinowitz J, Gitai Z, Wingreen N. 2014 Enzyme clustering accelerates processing of intermediates through metabolic channeling. *Nature Biotechnology* **32**, 1011–1018. (10.1038/nbt.3018)
49. Sweetlove L, Fernie A. 2018 The role of dynamic enzyme assemblies and substrate channelling in metabolic regulation. *Nature Communications* **9**, 2136. (10.1038/s41467-018-04543-8)
50. Kondrat S, von Lieres E. 2022 pp. 27–50. In *Mechanisms and Effects of Substrate Channelling in Enzymatic Cascades*, pp. 27–50. New York, NY: Springer US. (10.1007/978-1-0716-2269-8$_3$)
51. Bakker B, Mensonides F, Teusink B, van Hoek P, Michels P, Westerhoff H. 2000 Compartmentation protects trypanosomes from the dangerous design of glycolysis. *Proceedings of the National Academy of Sciences* **97**, 2087–2092. (10.1073/pnas.030539197)
52. Graham J, Williams T, Morgan M, Alisdair F, Ratcliffe R, Sweetlove L. 2007 Glycolytic enzymes associate dynamically with mitochondria in response to respiratory demand and support substrate channeling. *Plant Cell* **19**, 3723–3738.
53. Miura N, Shinohara M, Tatsukami Y, Sato Y, Morisaka H, Kuroda K, Ueda M. 2013 Spatial Reorganization of Saccharomyces cerevisiae Enolase To Alter Carbon Metabolism under Hypoxia. *Eukaryotic Cell* **12**, 1106–1119. (10.1128/ec.00093-13)
54. An S, Kumar R, Sheets E, Benkovic S. 2008 Reversible compartmentalization of de novo purine biosynthetic complexes in living cells. *Science* **320**, 103–106.
55. Macfadyen W. 1950 Vegetation patterns in the semi-desert plains of British Somaliland. *Geographical Journal* **116**, 199–211.
56. Dunkerley D. 2000 Hydrologic effects of dryland shrubs: defining the spatial extent of modified soil water uptake rates at an Australian desert site. *Journal of Arid Environments* **45**, 159–172. (https://doi.org/10.1006/jare.2000.0636)
57. Thompson SE, Harman CJ, Heine P, Katul GG. 2010 Vegetation-infiltration relationships across climatic and soil type gradients. *Journal of Geophysical Research: Biogeosciences* **115**. (https://doi.org/10.1029/2009JG001134)
58. HilleRisLambers R, Rietkerk M, Bosch F, Prins H, Kroon H. 2001 Vegetation Pattern Formation in Semi-Arid Grazing Systems. *Ecology* **82**, 50–61.
59. Siero E. 2020 Resolving soil and surface water flux as drivers of pattern formation in Turing models of dryland vegetation: A unified approach. *Physica D: Nonlinear Phenomena* **414**. (10.1016/j.physd.2020.132695)
60. Rietkerk M, Bastiaansen R, Banerjee S, van de Koppel J, Baudena M, Doelman A. 2021 Evasion of tipping in complex systems through spatial pattern formation. *Science* **374**, eabj0359. (10.1126/science.abj0359)
61. Turing A. 1952 The chemical basis of morphogenesis. *Philosophical Transactions of the Royal Society of London. Series B, Biological Sciences* **237**, 37–72.
62. Klausmeier C. 1999 Regular and irregular patterns in semi-arid vegetation. *Science* **284**, 1826–1828.
63. Bleichrodt RJ, Vinck A, Read ND, Wösten HAB. 2015 Selective transport between

heterogeneous hyphal compartments via the plasma membrane lining septal walls of Aspergillus niger. *Fungal Genet Biol* **82**, 193–200.
64. la Fuente ID, Cortes J, Malaina I, Pérez-Yarza G, Martinez L, López J, Fedetz M, Carrasco-Pujante J. 2025 The main sources of molecular organization in the cell. Atlas of self-organized and self-regulated dynamic biostructures. *Progress in Biophysics and Molecular Biology* **195**, 167–191. (https://doi.org/10.1016/j.pbiomolbio.2025.01.003)
65. Kauffman S. 1993 *The Origins of Order: Self-Organization and Selection in Evolution*. New York: Oxford University Press.
66. Karsenti E. 2008 Self-organization in cell biology: a brief history. *Nature Reviews Molecular Cell Biology* **9**, 255–262. (10.1038/nrm2357)
67. Kurakin A. 2009 Scale-free flow of life: on the biology, economics, and physics of the cell. *Theoretical Biology and Medical Modelling* **6**, 6. (10.1186/1742-4682-6-6)
68. Johnson B, Lam S. 2010 Self-organization, Natural Selection, and Evolution: Cellular Hardware and Genetic Software. *BioScience* **60**, 879–885. (10.1525/bio.2010.60.11.4)
69. de Jager M, Weissing F, van de Koppel J. 2017 Why mussels stick together: spatial self-organization affects the evolution of cooperation. *Evolutionary Ecology* **31**, 547–558. (10.1007/s10682-017-9888-1)
70. Kayser J, Schreck C, Yu Q, Gralka M, Hallatschek O. 2018 Emergence of evolutionary driving forces in pattern-forming microbial populations. *Philosophical Transactions of the Royal Society B: Biological Sciences* **373**, 20170106. (10.1098/rstb.2017.0106)
71. Doekes H, Hermsen R. 2024 Multiscale selection in spatially structured populations. *Proceedings of the Royal Society B: Biological Sciences* **291**, 20232559. (10.1098/rspb.2023.2559)